



## Research article

# Connexin 43 contributes to temporomandibular joint inflammation induced-hypernociception via sodium channel 1.7 in trigeminal ganglion

Yi-Zhou Jin<sup>a,b</sup>, Peng Zhang<sup>a,c</sup>, Ting Hao<sup>a,b</sup>, Lu-Ming Wang<sup>a,b</sup>, Mu-Di Guo<sup>a,b</sup>, Ye-Hua Gan<sup>a,b,\*</sup>

<sup>a</sup> Central Laboratory, Peking University School and Hospital of Stomatology, Beijing, PR China

<sup>b</sup> Department of Oral and Maxillofacial Surgery, Peking University School and Hospital of Stomatology, Beijing, PR China

<sup>c</sup> Department of Oral and Maxillofacial Surgery, Qingdao Municipal Hospital, Shandong, PR China



## ARTICLE INFO

## Keywords:

Inflammatory pain  
Trigeminal ganglion  
Sodium channel 1.7  
Satellite glial cells  
Connexin 43

## ABSTRACT

We previously demonstrated that sodium channel 1.7 (Nav1.7) in trigeminal ganglion (TG) was a critical factor in temporomandibular joint (TMJ) inflammation-induced hypernociception, but the mechanism underlying inflammation-induced upregulation of Nav1.7 remained unclear. Glial-neuron interaction plays a critical role in pain process and connexin 43 (Cx43), a gap junction protein expressed in satellite glial cells (SGCs) has been shown to play an important role in several pain models. In the present study, we investigate the role of Cx43 in TMJ inflammation-induced hypernociception and its possible impact on neuronal Nav1.7. We induced TMJ inflammation in rats by injecting complete Freund's adjuvant (CFA) into TMJ and observed a decrease in head withdraw threshold after 24 h. Electron microscopy showed morphological alterations of SGCs in TMJ-inflamed rats. The expression of Cx43, glial fibrillary acidic protein (GFAP), and Nav1.7 increased greatly compared with controls. In addition, pretreatment with Cx43 blockers in TMJ-inflamed rats could alleviate mechanical hypernociception, inhibit SGCs activation and IL-1 $\beta$  release, and thus block the upregulation of Nav1.7. These findings indicate that the propagation of SGCs activation via Cx43 plays a critical role in Nav1.7-involved mechanical hypernociception induced by TMJ inflammation.

## 1. Introduction

Temporomandibular joint (TMJ) inflammation-induced pain is characterized as pain in TMJ or masticatory muscles or both. However, the exact mechanism underlying inflammation-induced pain remains unclear.

Voltag e-g ated sodium channel 1.7 (Nav1.7), which is highly expressed in trigeminal ganglion (TG), amplifies weak stimuli in neurons and acts as the threshold channel for firing action potentials [1,2]. Accompanied by increased sodium currents amplitude [3], TMJ inflammation upregulated the protein expression of Nav1.7 as well [4–6]. Pretreatment with Nav1.7 antibody into TG could attenuate inflammation induced-hypernociception in TMJ region [4]. These results indicate that Nav1.7 plays an important role in the modulation of TMJ inflammatory pain.

In TG, the soma of sensory neuron is wrapped by satellite glial cells (SGCs), which could be identified by its morphological structure. Upregulation of glial fibrillary acidic protein (GFAP) is a useful marker for SGC activation [7]. While barely detectable in SGCs under physiological conditions, GFAP expression is dramatically elevated in

pathological conditions, such as systemic inflammation [8,9], peripheral nerve injury [10] and cancer [11].

Gap junctions, composed of two hemichannels, widely exist between adjacent cells in different tissues or organs. Each hemichannel is constituted of six connexins (Cx). Connexin 43 (Cx43) is the primary gap junction protein, known to modulate exchange of small molecules between cells [12]. Along with an upregulation of GFAP, the number of gap junctions in SGCs is also increased in several pain models [8,13]. Moreover, Cx43 in TG increased dramatically following inferior alveolar nerve transection (IANX), while blocking Cx43 could attenuate IANX-induced hypernociception in whisker pad skin [10]. These results imply that Cx43 in TG plays an important role in neuropathic pain conditions.

In this study, we examined morphologic alterations of SGCs in TG following TMJ inflammation. Changes in Cx43, GFAP and Nav1.7 expression were also examined. In addition, we investigated the functional significance of Cx43 in relation to mechanical hypernociception and Nav1.7 expression by administration of two different Cx43 blockers.

\* Corresponding author at: Central Laboratory, Peking University School and Hospital of Stomatology, Beijing, PR China.

E-mail address: [kqyehuagan@bjmu.edu.cn](mailto:kqyehuagan@bjmu.edu.cn) (Y.-H. Gan).

<https://doi.org/10.1016/j.neulet.2019.134301>

Received 30 March 2019; Received in revised form 27 May 2019; Accepted 28 May 2019

Available online 29 May 2019

0304-3940/ © 2019 Elsevier B.V. All rights reserved.

## 2. Materials and methods

### 2.1. Animals and induction of TMJ inflammation

Male Sprague-Dawley (SD) rats (220–280 g, Vital River Experimental Animal Technique Company, Beijing, China) were used in this study. All experiments were approved by Peking University Animal Ethics Committee (Approval number: LA2018325) and consistent with the Ethical Guidelines of the International Association for the Study of Pain. To induce TMJ inflammation, we injected 50  $\mu$ l complete Freund's adjuvant (CFA; Sigma, USA) (1:1 oil/saline emulsion) into bilateral TMJ of well-anesthetized rats (1% pentobarbital sodium, 40 mg/kg, i.p.) for 24 h as described in the previous study [14]. Rats which received 50  $\mu$ l incomplete Freund's adjuvant (IFA; Sigma, USA) (1:1 oil/saline emulsion) injection served as controls.

### 2.2. Behavioral testing

Head withdrawal threshold was associated with the mechanical sensitivity of the orofacial region [15] and was conducted as previously described [4]. Briefly, rats were trained to rear on their hindpaws and recline against experimenter's working gloves. Rats kept motionless during the test but were allowed to move freely. 2 h before and 24 h after the induction of TMJ inflammation, we applied the electronic von Frey filament (IITC Life Science, Woodland Hills, CA, USA) with the progressively increasing force on the skin of TMJ region. The applied force was automatically recorded at the moment the rat's head withdrew. The behavioral testing included at least five measurements per joint and four rats per group. The experimenters were blinded to the rats' treatment.

### 2.3. Intratrigeminal ganglionic injection

Well anesthetized rats (1% pentobarbital sodium, 40 mg/kg, i.p.) were mounted onto a stereotaxic frame (model 68001, RWD Life Science Company, Shenzhen, China). Two guide cannula (10 mm in length, 0.56 mm outer diameter and 0.32 mm inner diameter) were implanted into bilateral TG (3.5 mm posterior to the bregma, 3.6 mm lateral from the midline, and 9 mm ventral from the surface of the skull [16]) through a small hole drilled on the skull. Stainless screws and dental self-curing acrylic resin were used to fix the cannula onto the skull. A stainless steel stylet was inserted into the cannula to prevent obstruction or infection. After a 7-day recovery, the head withdrawal threshold (at least four rats per group) was measured to examine whether the implantation affected nociception. Microinjection of reagents into TG was performed through a 10  $\mu$ l Hamilton microsyringe (RWD Life Science Co., Ltd., Shenzhen, China) which was connected to a PE-10 polyethylene catheter with an inner cannula (12 mm in length, 0.3 mm outer diameter and 0.14 mm inner diameter). The inner cannula was specially designed and was extended by 2 mm beyond the end of the guide cannula. The injection process was performed at a rate of 0.2  $\mu$ l/min. Finally the rats were microinjected with 1  $\mu$ l of Evans blue to assess the accuracy of the injection site in the TG. The injection locations were evaluated by dissection.

### 2.4. Drugs administration

Carbenoxolone (CBX; Abcam, 100 mg/kg dissolved in saline) was injected (i.p.) in rats 30 min before CFA injection. Microinjection of Gap26 (Anaspec, 3 mM 10  $\mu$ l) was performed as described above at 24 h and 0.5 h before CFA injection. Doses of CBX and Gap26 were chosen on the basis of previously published work [17–19]. Rats received saline injection served as controls.

### 2.5. Transmission electron microscopy (TEM)

Animals were anaesthetized with 1% pentobarbital sodium (40 mg/kg, i.p.) and perfused transcardially with 3% glutaraldehyde in 0.1 M PBS. Several 1\*1\*2 mm sections were obtained from TGs and fixed in 3% glutaraldehyde overnight at 4°C. Then the sections were washed in 0.1 M PBS, postfixed in 2% OsO<sub>4</sub> in the same buffer. After subsequent washes in distilled water, the tissues were stained with uranyl acetate, dehydrated in ethanol and embedded in Epon-Araldite resin. After checking the quality of fixation, ultrathin sections were obtained from three control and three TMJ-inflamed ganglions and were further examined under transmission electron microscope (JEM-1400PLUS, Tokyo, Japan). For each section we determined: (a) the number of neurons surrounded by SGCs sheath; (b) the total number of gap junctions found between SGCs.

### 2.6. Western blot analysis

The dissection and homogenization of TGs and Western blot analysis were performed as described in detail previously [6]. The primary antibodies were as follows: anti-Nav1.7 antibody (1:1000, Proteintech), anti-COX-2 antibody (1:1000, CST), anti-phospho-CREB antibody (1:1000, CST), anti-CREB antibody (1:1000, CST), anti-IL-1 $\beta$  antibody (1:500, Abcam), anti-GFAP antibody (1:1000, CST), anti-Cx43 antibody (1:1000, Abcam) and anti- $\beta$ -actin antibody (1:10000, ZSGB-BIO). Densities were quantified by NIH ImageJ 1.38 software (NIH, Bethesda, MD, USA) and expressed as fold change of the control group after normalization to  $\beta$ -actin or CREB.

### 2.7. Immunofluorescence

Anesthetized rats were perfused and TG sections (6  $\mu$ m) were obtained as previously reported [5]. Sections were blocked with 10% goat serum for 30 min and then incubated with primary antibody (anti-Nav1.7, 1:300, Proteintech; anti-COX-2, 1:100, CST; anti-phospho-CREB, 1:50, CST; anti-IL-1 $\beta$ , 1:50, Abcam; anti-GFAP, 1:300, CST; anti-Cx43, 1:300, Abcam) overnight at 4°C. Sections were then labeled for 1 h with FITC goat anti-rabbit antibody (Jackson 1:200) or Alexa 488-CONjugated goat anti-mouse antibody (1:200, Jackson). After washes, the sections were coverslipped with diazobicyclooctane-containing glycerol. Confocal microscopic images were acquired using LSCM for further analysis.

### 2.8. Data analysis

Experimental data were analyzed with SPSS 20 for Windows (SPSS Inc., Chicago, IL, USA). All data was presented as mean  $\pm$  SD. Differences between two groups were examined by independent samples t test, whereas differences between groups were examined by one-way ANOVA test, followed by Tukey's multiple comparisons test. In all cases,  $P < 0.05$  was considered as statistically significant.

## 3. Results

### 3.1. TMJ inflammation resulted in ultrastructural alterations in SGCs

In the TG of either control or inflammation group, a single neuron soma was wrapped by several SGCs, named SGC sheath [7]. Occasionally, two or more neurons sharing a common SGC sheath was observed (Fig. 1a). Gap junctions could be found between SGCs comprising a single perineuronal sheath (Fig. 1b), but never been observed between neurons and its attendant satellite cells. As described in literature, the normal intercellular space reduced to 20 nm at gap junctions [20,21].

In control ganglions, all SGC sheaths had a rather smooth outer contour. Each sheath was totally separated from other sheath encircling

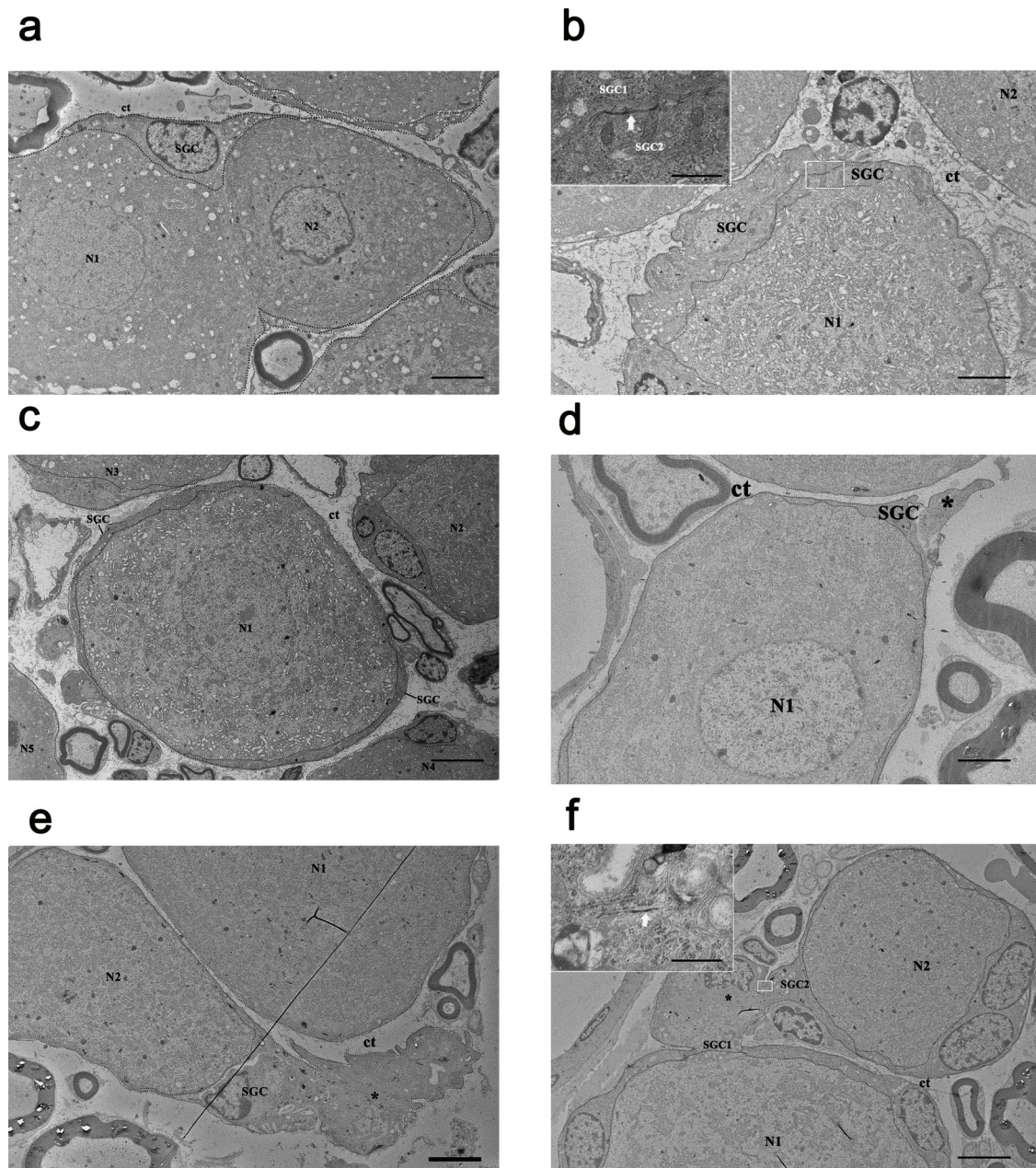


**Fig. 1.** Ultrastructural alterations of SGCs in TG after TMJ inflammation. **a** Two nerve cell bodies (N1, N2) sharing a common SGC sheath. **b** A gap junction (arrowhead) within a single perineuronal SGC sheath in the boxed area. The area is shown at higher magnification in the inset. **c** The outer contour of SGC sheath in control ganglion is rather smooth. Sheaths surrounding the adjacent nerve cell bodies (N1, N2, N3, N4, and N5) are completely separated by connective tissue (ct). **d**, **e** In TMJ-inflamed ganglions, asterisks point to cytoplasmic processes emerging from the outer contour of SGC sheath and projecting into the connective tissue space (ct). **f** A cytoplasmic bridge (asterisk) between two SGC sheaths. A gap junction (arrowhead) is shown at greater magnification in the inset. SGCs are outlined by dashed lines. Scale bar = 5  $\mu\text{m}$ ; inset: scale bar = 0.5  $\mu\text{m}$ .

adjacent neuron by connective tissue (ct) (Fig. 1c). In striking contrast, in ganglions from CFA-treated rats, the outer contour of SGC sheaths often showed elongated cytoplasmic processes emerging from SGCs and projecting into the connective tissue (Fig. 1d, e). At times, cytoplasmic processes from two adjacent SGC sheaths joined together, forming a cytoplasmic bridge between the two sheaths (Fig. 1f). Gap junctions were found in all bridges examined.

We examined 112 and 93 SGC sheaths enveloping a single neuron randomly from control and inflammation groups respectively, 15 (13.3%) and 39 (34.5%) gap junctions were found in two groups ( $P < 0.05$ ).

### 3.2. TMJ inflammation-induced mechanical hypernociception was accompanied by an increase of Cx43, GFAP and Nav1.7 expression

As found previously [4], at 24 h post-CFA injection there was a decrease in head withdraw threshold (Fig. 2a), suggesting that hypernociception ensued after TMJ inflammation. Protein expression of GFAP and Nav1.7 were significantly increased after induction of TMJ inflammation for 24 h (Fig. 2b, c). In addition, consistent with ultra-structure result, the expression of Cx43, a gap junction protein, was upregulated greatly (Fig. 2b, c). Confocal images showed the increase of Cx43-IR, GFAP-IR and Nav1.7-IR cells (Fig. 2d) and Cx43-IR, GFAP-IR cells were co-localized in SGCs (Fig. 2e).

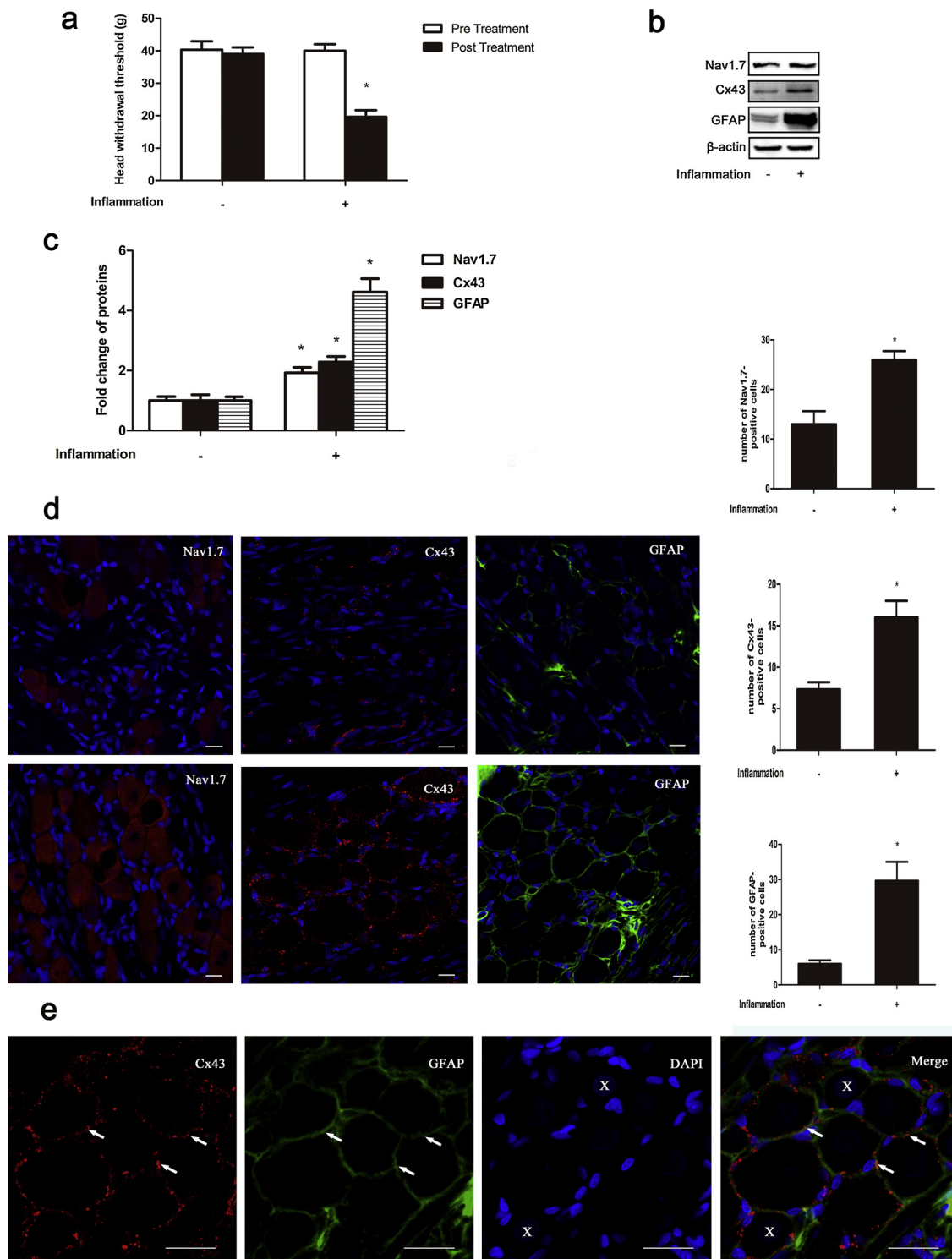


**Fig. 2.** Reduction of head withdrawal threshold and upregulation of Cx43, GFAP, Nav1.7 after TMJ inflammation for 24 h. **a** Decrease in head withdrawal threshold after TMJ inflammation. \* $P < 0.05$  versus control group,  $n = 4$ . **b** Representative immunoblotting shows the increase of Cx43, GFAP, and Nav1.7 expressions after TMJ inflammation.  $\beta$ -actin served as an internal control for equal loading. **c** Quantification of protein expressions are normalized against  $\beta$ -actin and presented as fold change of control group. \* $P < 0.05$  versus the control group,  $n = 3$ . **d, e** Confocal images show increase of Cx43-IR, GFAP-IR and Nav1.7-IR cells in TG after TMJ inflammation. Arrows denote double-IR cells. "X" denotes nucleus of neurons. The number of Cx43, GFAP and Nav1.7-IR cells is presented with histogram (right panel). \* $P < 0.05$  versus the control group,  $n = 3$ . Scale bar = 20  $\mu$ m.

**3.3. Cx43 blockers alleviated inflammatory hypernociception, as well as blocked inflammation-induced upregulation of Cx43, GFAP and Nav1.7**

Because SGCs gap junctions played an important role in several pain models [22] and its main component Cx43 was significantly

upregulated in the inflamed-TG, we asked whether Cx43 played a role in Nav1.7-mediated hypernociception. For this purpose, we applied two different Cx43 blockers.

We first applied nonspecific Cx43 blocker, carbenoxolone (CBX). All groups exhibited comparable head withdrawal threshold before drug

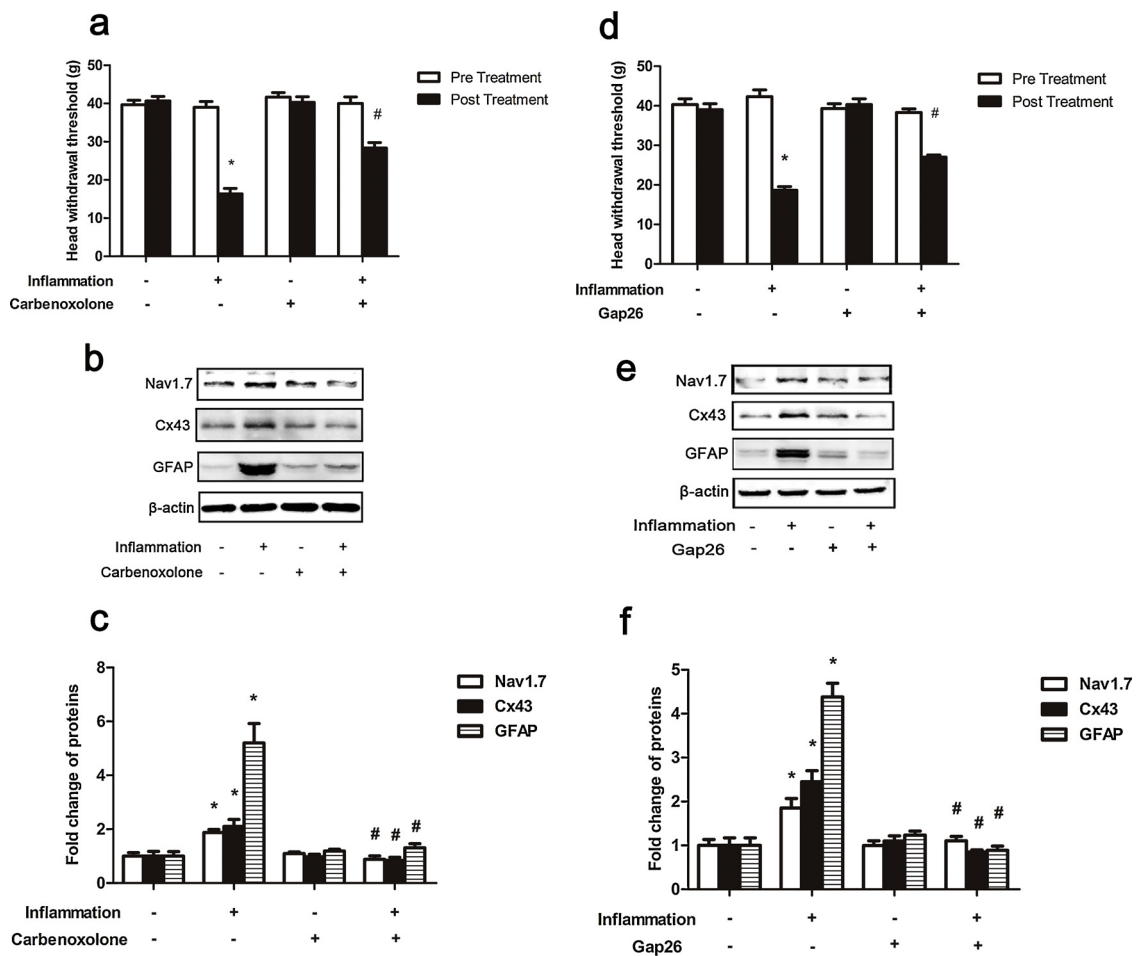


**Fig. 3.** Cx43 blockers attenuate hypernociception and block inflammation-induced upregulation of Cx43, GFAP and Nav1.7 in TG. **a, d** CBX/Gap26 partially inhibit TMJ inflammation-induced decrease in head withdrawal threshold. \* $P < 0.05$  versus control group. # $P < 0.05$  versus CFA group,  $n = 4$ . **b, e** Representative immunoblotting shows the inflammation-induced upregulation of Cx43, GFAP Nav1.7 is blocked by CBX/Gap26.  $\beta$ -actin served as an internal control for equal loading. **c, f** Quantification of protein expressions are normalized against  $\beta$ -actin and presented as fold change of control group. \* $P < 0.05$  versus the control group,  $n = 3$ ; # $P < 0.05$  versus CFA group,  $n = 3$ .

administration and CBX itself had no effect on pain threshold in non-inflamed rats. In contrast, CBX exerted attenuating effects on pain threshold of inflamed rats (Fig. 3a). Meanwhile, the inflammation-induced upregulation of Cx43, GFAP, and Nav1.7 was totally blocked by CBX (Fig. 3b, c).

We then applied specific Cx43 blocker, Gap26. Similar to CBX, microinjection of Gap26 in TG exhibited blocking function on head withdrawal threshold and inhibited the upregulation of Cx43, GFAP and Nav1.7 as well (Fig. 3d–f).

### 3.4. Suppression of IL-1 $\beta$ release could be one possible mechanism underlying Cx43 regulated Nav1.7-involved hypernociception

To explore the mechanisms underlying Cx43 contributed to hypernociception via Nav1.7, we tested cytokine release in SGCs. We previously reported that TMJ inflammation substantially increased the release of IL-1 $\beta$ , and then upregulated COX-2 in activated SGCs, resulted in upregulation of Nav1.7 expression via the neuronal CREB signaling pathway [5]. Notably, we found that pretreatment with CBX, as well as Gap26 suppressed the inflammation-induced IL-1 $\beta$  release and blocked the upregulation of downstream COX-2 and phospho-CREB (p-CREB) (Fig. 4a–d). Double-staining immunofluorescence images from TMJ-inflamed TG showed the location of IL-1 $\beta$ , COX-2 in activated SGCs, and p-CREB in nucleus of neurons (Fig. 4e–g), which was totally consistent with our previous finding [5].

## 4. Discussion

This study first demonstrates that Cx43 contributes to Nav1.7-involved mechanical hypernociception induced by TMJ inflammation. Our electron microscopic observations provided direct evidence for the morphological changes in SGCs after TMJ inflammation, including growth of cytoplasmic processes and formation of new gap junctions. Administration of Cx43 blockers significantly attenuated inflammation-induced hypernociception and blocked the upregulation of Cx43, GFAP and Nav1.7. In addition, we demonstrated that IL-1 $\beta$ -mediated neuron-glia interaction could be one possible mechanism underlying Cx43 regulated Nav1.7-involved hypernociception. These results might help us further understand the mechanisms underlying inflammatory pain and the regulation of trigeminal ganglionic Nav1.7 expression in inflammatory pain.

Our ultrastructure results are consistent with Hanani's finding in mice with LPS-induced systemic inflammation [8,9], showing the formation of cytoplasmic processes and the increase of SGCs gap junctions in dorsal root ganglion (DRG). The upregulation of Cx43 in TG has also been reported in the pain models of INAX and tooth pulp inflammation [10,17]. But another previous report claimed that in response to chronic or acute joint inflammation, the expression of Cx26, 36, 40 was upregulated but not including Cx43 [23]. This different result is probably due to the different time period post inflammation, for they tested the Cx43 expression on Day 3 after induction of TMJ inflammation. The

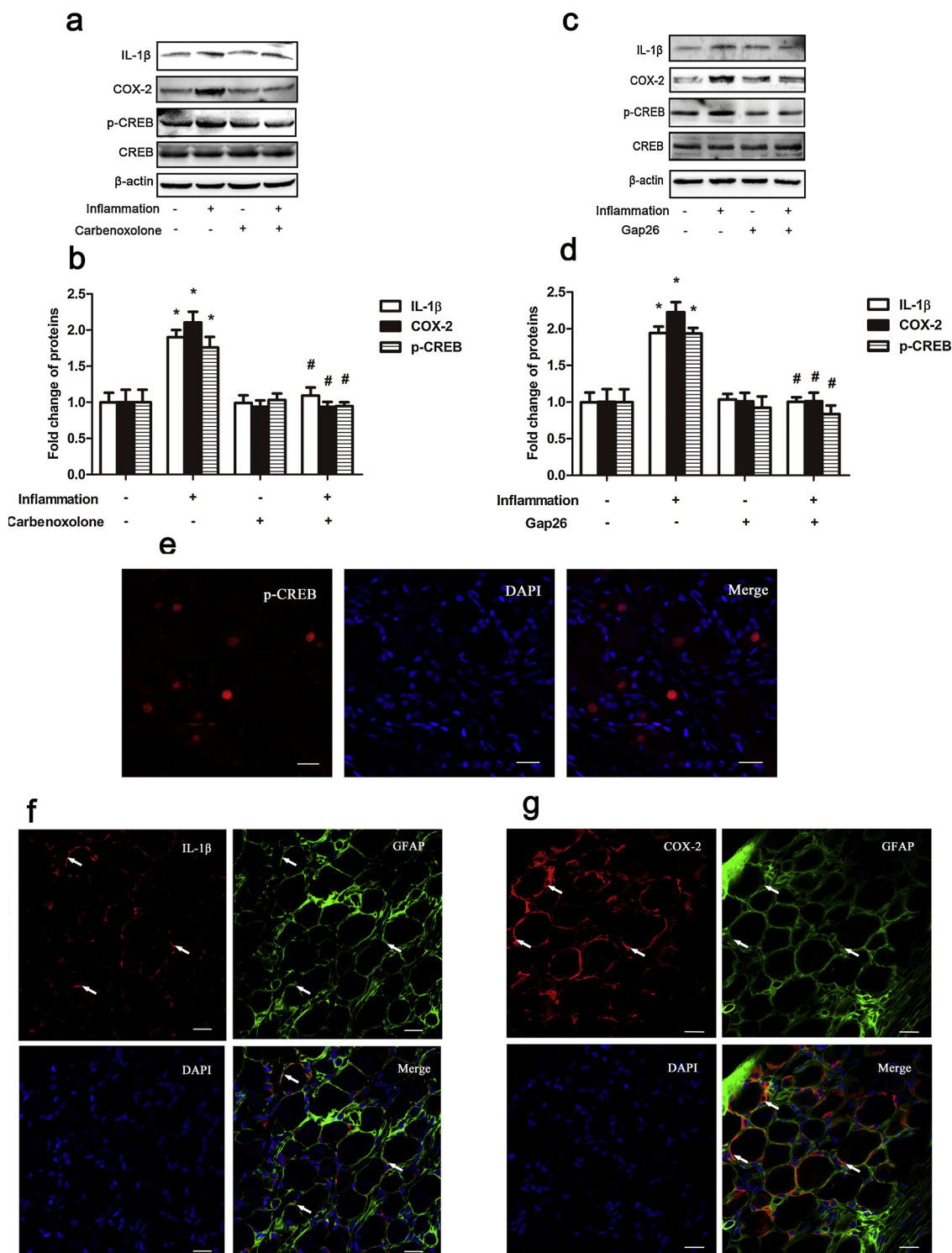


**Fig. 4.** Blocking function of CBX/Gap26 on Nav1.7 is attributed to the suppression of IL-1 $\beta$  release. **a, c** Representative immunoblotting shows that the inflammation-induced upregulation of IL-1 $\beta$ , COX-2, and p-CREB is inhibited by CBX/Gap26.  $\beta$ -actin served as an internal control for equal loading. **b, d** Quantification of protein expressions are normalized against  $\beta$ -actin or CREB and presented as fold change of control group. \* $P < 0.05$  versus the control group,  $n = 3$ ; # $P < 0.05$  versus CFA group,  $n = 3$ . **e-g** Confocal images of p-CREB-IR, IL-1 $\beta$ -IR, and COX-2-IR cells in TG on 24 h following induction of TMJ inflammation. Arrows denote double-IR cells. Scale bar = 20  $\mu$ m.

therapeutic effect of two Cx43 blockers in our study further supports the upregulation of Cx43.

The conclusion that hypernociception is attenuated by blocking Cx43 is based on the ability of CBX and Gap26 to block the function of Cx43. CBX, derived from glycyrrhetic acid, could produce an inhibition effect on gap junctional intercellular communication by disrupting

the configuration of the connexins, but without a selectivity for particular subtypes of Cx [24,25]. In addition, Gap26, targeted to the first extracellular loop of Cx43, could precisely block Cx43 hemichannel and thus affect the function of gap junctions. Besides TMJ inflammation, the fact that gap junction blockers have a therapeutic effect on pain has been reported in several other pain models, such as chemotherapy-

induced neuropathic pain [19] and systemic inflammation-related pain [8,9], suggesting that its effects are general to various pain states. But the mechanism underlying gap junction blockers attenuate hypernociception remains unclear. In exploring the mechanisms underlying TMJ inflammation induced hypernociception, our previous study focused on the role of neuronal Nav1.7. Several recent work illustrate the importance of glial cells in the occurrence and development of hypernociception, and demonstrate that glial-neuron interactions play a critical role in pain process [22]. The most interesting part of our study is that we find a relationship between Cx43 in SGCs and Nav1.7 in neurons. For the very first time, we demonstrate that TMJ inflammation-induced upregulation of Nav1.7 is dependent on the function of Cx43 in SGCs. Importantly, we note that when CBX/ Gap26 is applied into control animals, it has no influence on pain behavior or on Nav1.7 expression. Therefore, it is probably that CBX/ Gap26 acts largely when Cx43 is augmented, as occurred in several pain models, including TMJ inflammation.

Previously we showed that IL-1 $\beta$ , released from activated SGCs, was involved in Nav1.7 expression enhancement through COX-2/PGE2/EP2-evoked PKA/CREB signaling pathway in response to TMJ inflammation [5]. K. Shimizu's group has also reported the role of IL-1 $\beta$ -mediated neuron-glia interaction in hypernociception. The result that inflammation-induced increase of IL-1 $\beta$ , COX-2 and p-CREB is blocked by CBX/ Gap26 suggests that IL-1 $\beta$ -mediated interactions could be one possible mechanism underlying Cx43 regulates Nav1.7-involved hypernociception.

It is necessary to mention that though the upregulation of Cx43, GFAP and Nav1.7 was completely blocked by Cx43 blockers, the hypernociception was only partially attenuated. So there may exist direct effect on neurons underlying TMJ inflammation-induced hypernociception which needs further study.

In conclusion, the involvement of trigeminal ganglionic Nav1.7 in the hyperalgesia of the inflamed TMJ is dependent on the function of Cx43 in SGCs. Our results may help further understand the role of gap junctions in hypernociception and develop a new strategy to deal with inflammation-related pain.

#### Authors contributions

Yi-Zhou Jin, Peng Zhang, Ting Hao, Lu-Ming Wang, Mu-Di Guo carried out animal and laboratory experiments. Yi-Zhou Jin analyzed the data, and wrote the manuscript. Ye-Hua Gan contributed to the concept and design of the study, the coordination of all experiments, and critical review of the manuscript. Both authors read and approved the final manuscript.

#### Conflict of interest

The authors declare that they have no competing financial interests.

#### Acknowledgements

This work was supported by the National Natural Science Foundation of China (Grant No. 81271173) and China International Science and Technology Cooperation (Grant No. 2013DFB30360).

#### References

- [1] Theodore R. Cummins, James R. Howe, Stephen G. Waxman, Slow closed-state inactivation: a novel mechanism underlying ramp currents in cells expressing the hNE/PN1 sodium channel, *J. Neurosci.* 18 (1998) 9607–9619.
- [2] S.G. Waxman, Neurobiology: a channel sets the gain on pain, *Nature* 444 (2006) 831–832.
- [3] N.M. Flake, M.S. Gold, Inflammation alters sodium currents and excitability of temporomandibular joint afferents, *Neurosci. Lett.* 384 (2005) 294–299.
- [4] R.Y. Bi, X.X. Kou, Z. Meng, X.D. Wang, Y. Ding, Y.H. Gan, Involvement of trigeminal ganglionic Nav 1.7 in hyperalgesia of inflamed temporomandibular joint is dependent on ERK1/2 phosphorylation of glial cells in rats, *Eur. J. Pain* 17 (2013) 983–994.
- [5] P. Zhang, R.Y. Bi, Y.H. Gan, Glial interleukin-1beta upregulates neuronal sodium channel 1.7 in trigeminal ganglion contributing to temporomandibular joint inflammatory hypernociception in rats, *J. Neuroinflammation* 15 (2018) 117–133.
- [6] P. Zhang, Y.H. Gan, Prostaglandin E2 upregulated trigeminal ganglionic sodium channel 1.7 involving temporomandibular joint inflammatory pain in rats, *Inflammation* 40 (2017) 1102–1109.
- [7] M. Hanani, Satellite glial cells in sensory ganglia: from form to function, *Brain Res. Brain Res. Rev.* 48 (2005) 457–476.
- [8] E. Blum, P. Procacci, V. Conte, M. Hanani, Systemic inflammation alters satellite glial cell function and structure, A possible contribution to pain, *Neuroscience* 274 (2014) 209–217.
- [9] E. Blum, P. Procacci, V. Conte, P. Sartori, M. Hanani, Long term effects of lipopolysaccharide on satellite glial cells in mouse dorsal root ganglia, *Exp. Cell Res.* 350 (2017) 236–241.
- [10] K. Kaji, M. Shinoda, K. Honda, S. Unno, N. Shimizu, K. Iwata, Connexin 43 contributes to ectopic orofacial pain following inferior alveolar nerve injury, *Mol. Pain* 12 (2016) 1–12.
- [11] Katsunori Hironaka, H.ideyuki Nakashima, H.isashi Hattori, M.inoru ueda, Kenjiro Nagamine, Yasuo Sugiura, Involvement of glial activation in trigeminal ganglion in a rat model of lower gingival cancer pain, *Najoya J. Med. Sci.* 76 (2014) 323–332.
- [12] M.J. Chen, B. Kress, X. Han, K. Moll, W. Peng, R.R. Ji, M. Nedergaard, Astrocytic CX43 hemichannels and gap junctions play a crucial role in development of chronic neuropathic pain following spinal cord injury, *Glia* 60 (2012) 1660–1670.
- [13] E. Pannese, M. Ledda, P.S. Cherkas, T.Y. Huang, M. Hanani, Satellite cell reactions to axon injury of sensory ganglion neurons: increase in number of gap junctions and formation of bridges connecting previously separate perineuronal sheaths, *Anat Embryol (Berl)* 206 (2003) 337–347.
- [14] Y.W. Wu, Y.P. Bi, X.X. Kou, W. Xu, L.Q. Ma, K.W. Wang, Y.H. Gan, X.C. Ma, 17-Beta-estradiol enhanced allodynia of inflammatory temporomandibular joint through upregulation of hippocampal TRPV1 in ovariectomized rats, *J. Neurosci.* 30 (2010) 8710–8719.
- [15] K. Ren, An improved method for assessing mechanical allodynia in the rat, *Physiol. Behav.* 67 (1999) 711–716.
- [16] Tang Xiu Feng, Bi Rui Yun, Meng Zhen, Gan Ye Hua, Stereotaxis of mandibular nerve initial point of trigeminal ganglion in rats, *Chin. J. Dent. Res.* 17 (2014) 99–104.
- [17] H. Komiya, K. Shimizu, K. Ishii, H. Kudo, T. Okamura, K. Kanno, M. Shinoda, B. Ogiso, K. Iwata, Connexin 43 expression in satellite glial cells contributes to ectopic tooth-pulp pain, *J. Oral Sci.* 60 (2018) 493–499.
- [18] H. Diao, S. Xiao, E.W. Howerth, F. Zhao, R. Li, M.B. Ard, X. Ye, Broad gap junction blocker carbenoxolone disrupts uterine preparation for embryo implantation in mice, *Biol. Reprod.* 89 (2013) 1–10.
- [19] R.A. Warwick, M. Hanani, The contribution of satellite glial cells to chemotherapy-induced neuropathic pain, *Eur. J. Pain* 17 (2013) 571–580.
- [20] J.P.Ra.M.J. Karnovsky, Hexagonal array of subunits in intercellular junctions of mouse heart and liver, *J. Cell Biol.* 33 (1967) 7–12.
- [21] T.S.R.M.W. Brightman, Junctions between intimately apposed cell membranes in the vertebrate brain, *J. Cell Biol.* 40 (1969) 648–677.
- [22] D.C. Spray, M. Hanani, Gap junctions, pannexins and pain, *Neurosci. Lett.* 695 (2017) 46–52.
- [23] F.G. Garrett, P.L. Durham, Differential expression of connexins in trigeminal ganglion neurons and satellite glial cells in response to chronic or acute joint inflammation, *Neuron Glia Biol.* 4 (2008) 295–306.
- [24] J.S. Davidson, I.M. Baumgarten, E.H. Harley, Reversible inhibition of intercellular junctional communication by glycyrrhetic acid, *Biochem. Biophys. Res. Commun.* 134 (1986) 29–36.
- [25] J.S. Davidson, I.M. Baumgarten, Glycyrrhetic acid derivatives: a novel class of inhibitors of gap-junctional intercellular communication. Structure-activity relationships, *J. Pharmacol. Exp. Ther.* 246 (1988) 1104–1107.